The dual pathway in action: decoupling parallel routes for CO2 production during the oscillatory electro-oxidation of methanol

PHYSICAL CHEMISTRY CHEMICAL PHYSICS, CAMBRIDGE, v. 14, n. 23, supl. 1, Part 3, pp. 8294-8298, OCT, 2012
http://www.producao.usp.br/handle/BDPI/36668

PCCP

Physical Chemistry Chemical Physics

www.rsc.org/pccp

Volume 14 | Number 23 | 21 June 2012 | Pages 8241–8436

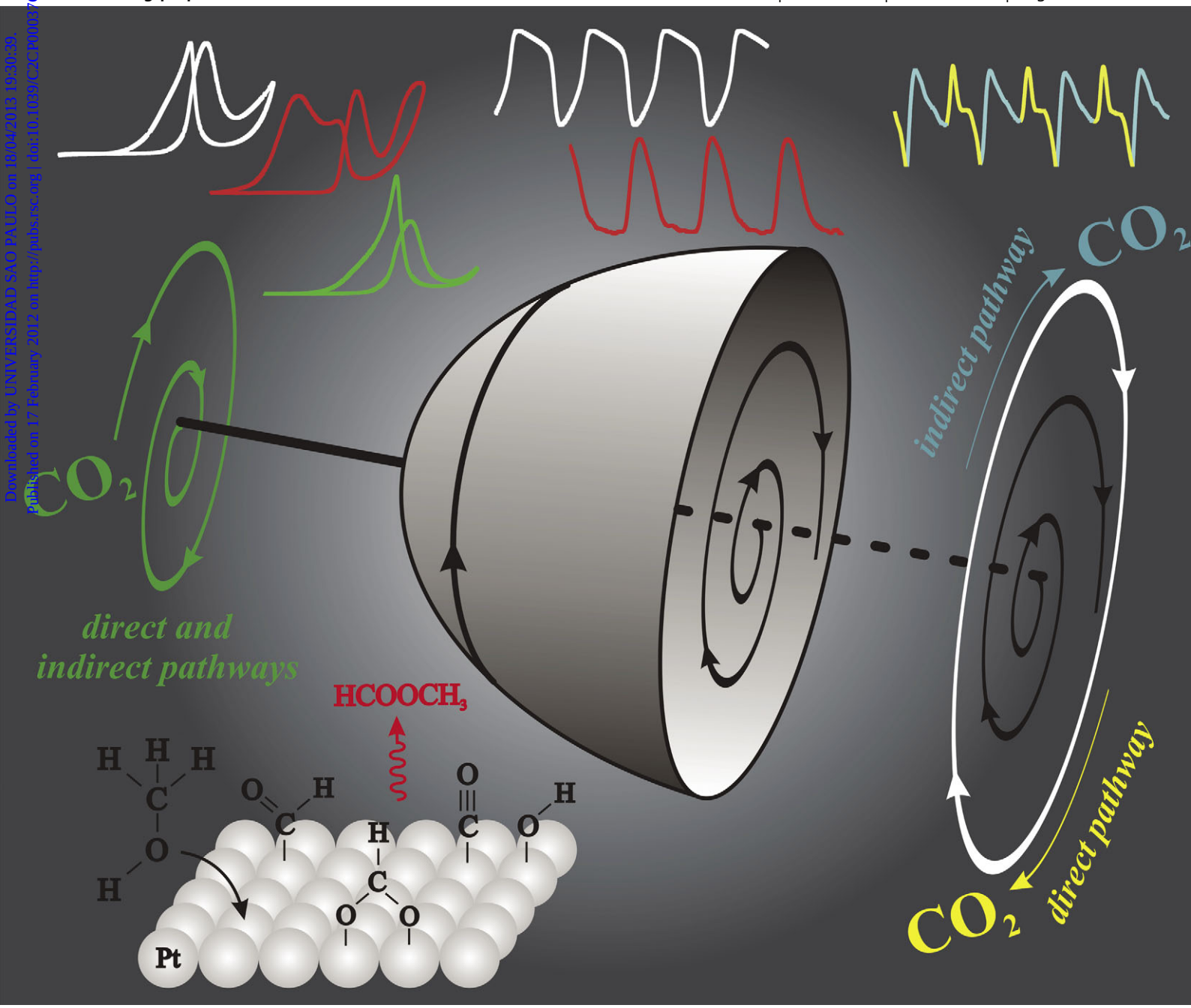

ISSN 1463-9076

COVER ARTICLE

Varela *et al.*

The dual pathway in action: decoupling parallel routes for CO_2 production during the oscillatory electro-oxidation of methanol

1463-9076(2012)14:23;1-T

PCCP

Dynamic Article Links
View Article Online

Cite this: *Phys. Chem. Chem. Phys.*, 2012, **14**, 8294–8298

www.rsc.org/pccp

PAPER

The dual pathway in action: decoupling parallel routes for CO_2 production during the oscillatory electro-oxidation of methanol

Raphael Nagao,[a] Daniel A. Cantane,[a] Fabio H. B. Lima[a] and Hamilton Varela*[ab]

Received 5th January 2012, Accepted 16th February 2012
DOI: 10.1039/c2cp00037g

As in the case of most small organic molecules, the electro-oxidation of methanol to CO_2 is believed to proceed through a so-called dual pathway mechanism. The direct pathway proceeds *via* reactive intermediates such as formaldehyde or formic acid, whereas the indirect pathway occurs in parallel, and proceeds *via* the formation of adsorbed carbon monoxide (CO_{ad}). Despite the extensive literature on the electro-oxidation of methanol, no study to date distinguished the production of CO_2 from direct and indirect pathways. Working under, far-from-equilibrium, oscillatory conditions, we were able to decouple, for the first time, the direct and indirect pathways that lead to CO_2 during the oscillatory electro-oxidation of methanol on platinum. The CO_2 production was followed by differential electrochemical mass spectrometry and the individual contributions of parallel pathways were identified by a combination of experiments and numerical simulations. We believe that our report opens some perspectives, particularly as a methodology to be used to identify the role played by surface modifiers in the relative weight of both pathways—a key issue to the effective development of catalysts for low temperature fuel cells.

Introduction

As in the case of most small organic molecules, the electro-oxidation of methanol to CO_2 is believed to proceed through a parallel, dual pathway mechanism.[1,2] The direct pathway progresses *via* reactive intermediates such as formaldehyde or formic acid. The indirect pathway occurs in parallel, and proceeds *via* the formation of adsorbed carbon monoxide (CO_{ad}), which reacts with adsorbed oxygenated species at high potentials *via* a Langmuir–Hinshelwood mechanism in the Ertl reaction.[3] Despite the extensive literature on the electro-oxidation of methanol,[4–14] the activity of the direct pathway for methanol electro-oxidation is generally followed by the production of methylformate,[6] and no study to date distinguished the production of CO_2 from direct and indirect pathways.

Herein we report the accomplishment of this goal and unambiguously show the dual pathway mechanism in action. Electrochemical oscillations were followed *on line* by means of Differential Electrochemical Mass Spectrometry (DEMS). Unlike previous investigations on the oscillatory dynamics using *on line* DEMS[15,16] the present report brings rather unexpected results that provide new insight on the reaction mechanism. Indeed, working under far-from-equilibrium conditions, we were able to decouple the direct and indirect pathways that lead to CO_2 during the oscillatory electro-oxidation of methanol on platinum. The experimental results are interpreted and validated by modeling and numerical simulations.

Experimental

The working electrode was a platinum sputtered Teflon membrane (Gore-Tex, PTFE) with a thickness of around 50 nm, and with a real area of 3.9 cm^2 and roughness of 9.7, as measured by means of CO stripping. A high area platinized-platinum electrode and a reversible hydrogen electrode served as counter and reference electrodes, respectively. All electrochemical experiments were performed in solutions prepared with high purity water (Milli-Q, 18.2 MΩ cm), $HClO_4$ (Sigma-Aldrich, 71%), H_3COH (J. T. Baker, 99.9%) and controlled by the potentio/galvanostat (Autolab, PGSTAT 30). The cell temperature was kept constant at 20.0 ± 0.1 °C with the aid of a Cole–Parmer Polystat temperature controller. The DEMS apparatus was adapted to an electrochemical cell through a two chamber system (Pfeiffer, Vacuum) in order to obtain a fast *on line* temporal resolution. A quadrupole/Faraday cup/electron multiplier (Pfeiffer, QMA 200) was utilized as analyzer and the mass/charge (m/z) ratios 44 (carbon dioxide) and 60 (methylformate) were monitored with a data acquisition frequency of 5.7 Hz. The electrochemical data were measured at 10 Hz.

The faradaic and mass currents were normalized by CO stripping charge and $[CO_2]^+$ mass signal, respectively. In order to estimate the response time of the DEMS apparatus, we used the method suggested by Wolter and Heitbaum.[17]

[a] *Institute of Chemistry of São Carlos, University of São Paulo CP 780, CEP 13560-970, São Carlos, SP, Brazil. E-mail: varela@iqsc.usp.br*
[b] *Ertl Center for Electrochemistry and Catalysis, GIST Cheomdan-gwagiro 261, Buk-gu, Gwangju 500-712, South Korea*

The sputtered Pt electrode was subjected to a potential step from 0.4 to −0.1 V *vs.* RHE and then moved back to 0.4 V after 30 s, while the $m/z = 2$ signal (H_2) was simultaneously measured. With the step to −0.1 V, hydrogen is evolved and the $m/z = 2$ signal follows the cathodic current. The obtained curves for faradaic and ionic currents resulted in a stepped function. The software was set to read the hydrogen signal each 2 ms. After accounting for the delay time of the potentiostat response (0.04 s), the obtained results showed that the response time of the m/z signal was close to 0.03–0.05 s. So that, we can safely state that the mass fragments followed here are detected less than 0.10 s later than the electrochemical signal. After each galvanostatic experiment the system was left to relax to its open circuit potential (*i.e.* ~0.33 V) during one minute, enough time to get a good base line. From this reference we normalized the mass signal magnitude as zero current. Both mass signals were recorded simultaneously along the electrochemical data. The following protocol was applied prior to galvanostatic experiments: 10 cycles between 0.05 and 1.5 V at 0.10 V s^{-1} (ending at 0.05 V) followed by a current step to the desired value and then, after the measurement, the electrochemical cell was kept under open circuit conditions for one minute. This procedure assured a very good reproducibility and allowed us to define a base line as a mass normalization criterion; a similar procedure was adopted by Seidel *et al.*[16]

Modeling

Fig. 1 summarizes the, currently accepted, main aspects of the parallel pathways for the electro-oxidation of methanol on platinum. After initial adsorption and partial dehydrogenation, adsorbed methanol residues can be oxidized in parallel routes, *i.e.* the direct (non-CO) and indirect (CO) pathways. Adsorbed formic acid might either act as a precursor for adsorbed formate, an intermediate in the direct pathway,[9,18,19] or desorb from the surface. Dissolved HCOOH can adsorb again, generating formate in a fast equilibrium. Instead of being formed in the homogeneous reaction between formic acid and methanol,[10,13] methylformate is now believed to be formed *via* the nucleophilic attack of a methanol molecule on an adsorbed intermediate,[20] HCO_{ad} in Fig. 1. Bridge-bonded adsorbed formate can decompose to carbon dioxide[19,21,22] or to CO_{ad} by a reduction step,[23] both requiring an additional active surface site for the C–H breaking.

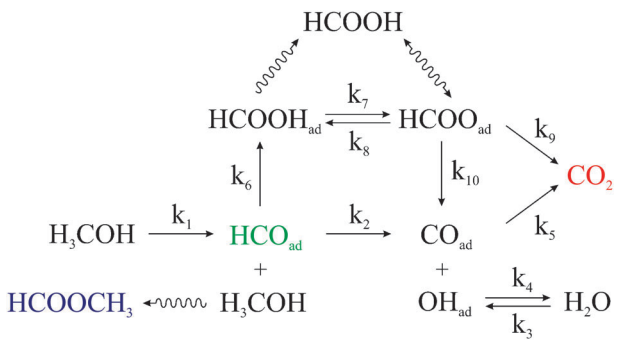

Fig. 1 Modeling elementary reaction steps for the methanol electro-oxidation.

The steps summarized in Fig. 1 are detailed in reactions (r1) to (r10) as follows:

$$H_3COH + 3* \xrightarrow{k_1} HCO_{ad} + 3H^+ + 3e^- \quad (r1)$$

$$HCO_{ad} \xrightarrow{k_2} CO_{ad} + H^+ + e^- + 2* \quad (r2)$$

$$H_2O + * \xrightarrow{k_3} OH_{ad} + H^+ + e^- \quad (r3)$$

$$OH_{ad} + H^+ + e^- \xrightarrow{k_4} H_2O + * \quad (r4)$$

$$CO_{ad} + OH_{ad} \xrightarrow{k_5} CO_2 + H^+ + e^- + 2* \quad (r5)$$

$$HCO_{ad} + * + H_2O \xrightarrow{k_6} HCOOH_{ad} + H^+ + e^- + 2* \quad (r6)$$

$$HCOOH_{ad} \xrightarrow{k_7} HCOO_{ad} + H^+ + e^- \quad (r7)$$

$$HCOO_{ad} + H^+ + e^- \xrightarrow{k_8} HCOOH_{ad} \quad (r8)$$

$$HCOO_{ad} + * \xrightarrow{k_9} CO_2 + H^+ + e^- + 3* \quad (r9)$$

$$HCOO_{ad} + * + H^+ + e^- \xrightarrow{k_{10}} CO_{ad} + H_2O + 2* \quad (r10)$$

These steps were translated into a mathematical model consisting of six ordinary differential equations (ODEs) accounting for the time evolution of HCO_{ad}, OH_{ad}, CO_{ad}, $HCOOH_{ad}$, $HCOO_{ad}$ and the electrode potential, ϕ. The variables were written as x_n according to: $x_2 = \theta_{HCO}$, $x_3 = \theta_{OH}$, $x_4 = \theta_{CO}$, $x_5 = \theta_{HCOOH}$, and $x_6 = \theta_{HCOO}$. j might be interpreted as the total applied current, $x_e = e^{\omega\phi}$ as the electrical component for faradaic reactions and ω as the transfer coefficient. The surface free sites are denoted as x_1 that reads:

$$x_1 = 1 - 3x_2 - x_3 - x_4 - 2x_5 - 2x_6$$

The reaction rates of the elementary steps are:

$$v_1 = k_1 x_1^2 x_e \quad (e1)$$

$$v_2 = k_2 x_2 x_e \quad (e2)$$

$$v_3 = k_3 x_1 x_e \quad (e3)$$

$$v_4 = k_4 x_3 x_e^{-1} \quad (e4)$$

$$v_5 = k_5 x_3 x_4 x_e \quad (e5)$$

$$v_6 = k_6 x_1 x_2 x_e \quad (e6)$$

$$v_7 = k_7 x_5 x_e \quad (e7)$$

$$v_8 = k_8 x_6 x_e^{-1} \quad (e8)$$

$$v_9 = k_9 x_1 x_6 x_e \quad (e9)$$

$$v_{10} = k_{10} x_1 x_6 x_e^{-1} \quad (e10)$$

The use of two free platinum sites in eqn (e1) follows the approximation adopted in ref. 24. In order to simplify the model, we also kept x_e as a function independent of the number of electrons produced in each elementary step.

The set of ordinary differential equations used in our simulations are given by the set (e11) to (e16):

$$\dot{x}_2 = v_1 - v_2 - v_6 \quad \text{(e11)}$$

$$\dot{x}_3 = v_3 - v_4 - v_5 \quad \text{(e12)}$$

$$\dot{x}_4 = v_2 - v_5 + v_{10} \quad \text{(e13)}$$

$$\dot{x}_5 = v_6 - v_7 + v_8 \quad \text{(e14)}$$

$$\dot{x}_6 = v_7 - v_8 - v_9 - v_{10} \quad \text{(e15)}$$

$$\dot{\Phi} = j - v_F \quad \text{(e16)}$$

with:

$$v_F = 3v_1 + v_2 + v_3 - v_4 + v_5 + v_6 + v_7 - v_8 + v_9 - v_{10} \quad \text{(e17)}$$

The six nonlinear, coupled ODEs were numerically integrated using the tool NDSolve in the Mathematica software.

Results and discussion

Fig. 2 depicts the voltammetric characterization of our system in terms of (a) the faradaic current density, and the variations in the mass fragments (b) $m/z = 44$ (carbon dioxide) and (c) 60 (methylformate), obtained at 0.01 V s^{-1}. Overall, the general features of these three voltammetric profiles are in agreement with previously published data.[25,26]

As in the case of many small organic molecules,[27] the electro-oxidation of methanol is known to display potential/current oscillations under some circumstances.[28–37] Fig. 3 shows

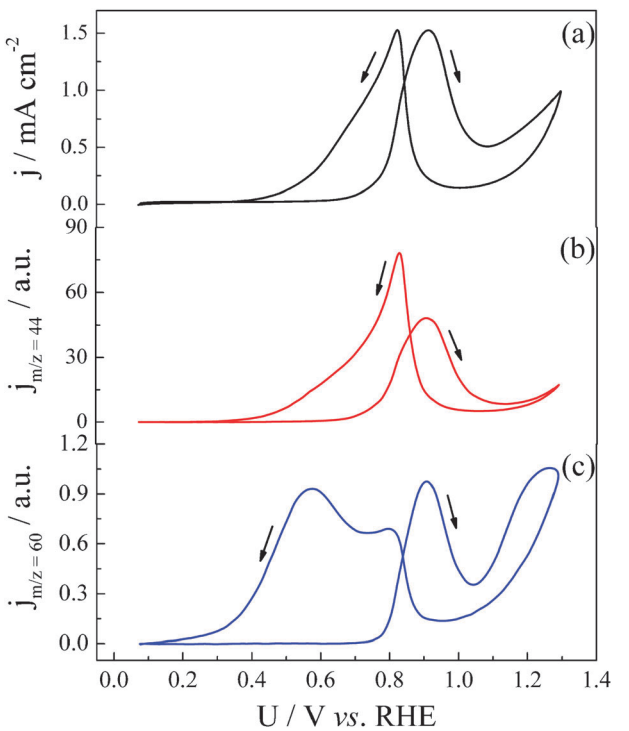

Fig. 2 Simultaneously recorded (a) cyclic voltammogram at 0.01 V s^{-1} and mass fragments of m/z = (b) 44 and (c) 60 for a platinum sputtered electrode. $[H_3COH]$ = 2.0 mol L^{-1}, $[HClO_4]$ = 0.5 mol L^{-1} and T = 20 °C.

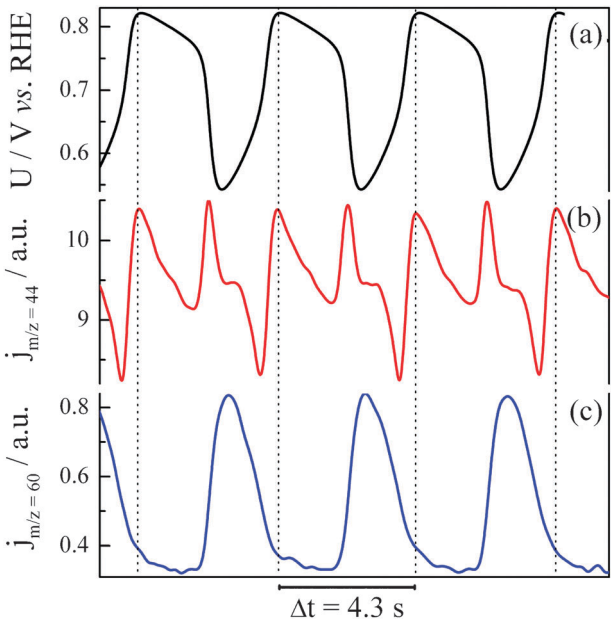

Fig. 3 Time-series for: (a) potential at j = 0.35 mA cm^{-2} during methanol electro-oxidation in perchloric acid accompanied by the mass fragments of m/z = (b) 44 and (c) 60. $[H_3COH]$ = 2.0 mol L^{-1}, $[HClO_4]$ = 0.5 mol L^{-1} and T = 20 °C.

typical time-series registered at j = 0.35 mA cm^{-2} for the (a) electrode potential and the mass fragments (b) 44 and (c) 60. The maximum delay estimated for the mass detection (<0.10 s) is considerably smaller than the oscillation period (*ca.* 4.3 s), so that the as-recorded time-series in Fig. 3 can be considered synchronized for practical purposes.

The main aspect to be pointed out in Fig. 3 is certainly the presence of additional peaks for the CO_2 production for each potential oscillation. This is in rather contrast also to the regular period-one related to harmonic and out-of-phase oscillations found for the $HCOOCH_3$ mass fragment. The fact that the complex waveform for the CO_2 production does not match the relatively simple period-one oscillations of the electrode potential and for the methylformate formation is a hint that this signal actually accounts for more than one elementary step. This is the main aspect of our contribution and will be developed in the following. The conjecture that the CO_2 production comes only partially from the oxidation of CO_{ad} is in line with our recent finding using *in situ* IR-spectroscopy,[36] in the sense that a period-one oscillation profile was found for the coverage of CO_{ad}, and similar conditions.

The integration of eqn (e11) to (e16) resulted in oscillations for several combinations of rate constants, a typical simulated time-series is illustrated in Fig. 4. The simulated profiles for the (a) electrode potential and (b) the overall CO_2 production can be compared to the experimentally obtained results given in Fig. 3(a) and (b), respectively. Following the scheme depicted in Fig. 1, the concentration of adsorbed HCO can be though as proportional to the concentration of dissolved methylformate. Comparing the relative phases for the electrode potential and methylformate time-series for simulations, Fig. 4(a) and (c), and experiments, Fig. 3(a) and (c) evidence

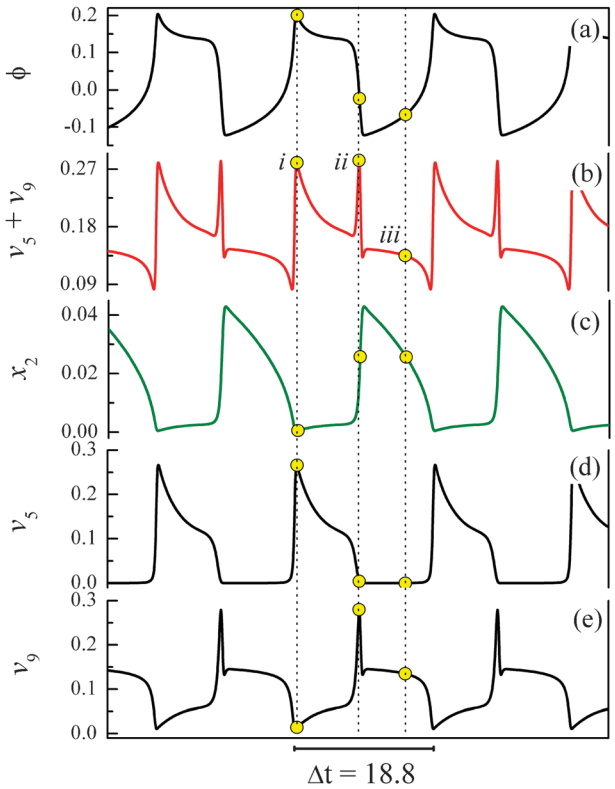

Fig. 4 Simulated time-series using eqn (e11) to (e16) for: (a) ϕ, double-layer potential; (b) $v_5 + v_9$, total CO_2; (c) x_2, HCO coverage; (d) v_5, CO_2 from indirect and (e) v_9, CO_2 from direct pathway. Simulations were carried out using the following rate constants: $k_1 = 6$, $k_2 = 5$, $k_3 = 1$, $k_4 = 4$, $k_5 = 0.079$, $k_6 = 50$, $k_7 = 600$, $k_8 = 30$, $k_9 = 300$, $k_{10} = 0.1$, $\omega = 15$ and $j = 1$.

a conspicuous correspondence and in both cases the methyl-formate production remains out-of-phase with the electrode potential.

Focusing now on the time-series for the CO_2 production, Fig. 4(b), peaks *i* and *ii* have comparable phase with respect to the potential time trace and relative amplitudes to that observed in experiments, Fig. 3(b). The small shoulder assigned as *iii* develops at relatively small amplitude and it is somewhat more separated from peak *ii*, when compared to that observed in experiments, Fig. 3(b). Despite this small discrepancy, the minimum value for the CO_2 production in both experiments and simulations seems to coincide.

Given the good congruence between experiments and simulations, the experimental results can be consistently interpreted now. The main point is the complex overall CO_2 production results of the sum of two parallel contributions: the indirect and the direct pathway, as evidenced by the decomposition of the global signal, Fig. 4(b), into the two individual ones, Fig. 4(d) and (e). The CO_2 production *via* CO_{ad}, Fig. 4(d), occurs in-phase with the oscillation in the electrode potential and the maxima for both profiles coincide. In the direct pathway, Fig. 4(e), the highest CO_2 production occurs very steeply during the decrease of the electrode potential and also coincides with the raising part of production of adsorbed HCO.

There is a general agreement that the electro-oxidation of methanol on platinum proceeds *via* a parallel or dual pathway mechanism. At low overpotentials, CO_{ad} is very stable and the direct oxidation dominates. At high overpotentials, where CO_{ad} is readily oxidized, both pathways become important and occur in parallel. Although convincing, the evidence for this mechanism is indirect and only the overall production of CO_2 has been followed to date. Working under, far-from-equilibrium, oscillatory conditions, we were able to decouple the parallel direct and indirect pathways measuring a common product from both routes (*i.e.* CO_2).

Self-organized chemical states at the solid–gas interface have revealed a myriad of enticing phenomena and also helped us to understand fundamental questions.[38] Examples as the one reported here might inspire experimental and theoretical efforts and contribute, for instance, to uncover mechanistic aspects of chemical phenomena occurring at the electrified solid–liquid interface. In the light of our results, the previously published model[24] for the oscillatory electro-oxidation of methanol must be revised in order to include, at least, both direct and indirect pathways. Our results can be also viewed as a methodology, and be employed as a precise means to identify the role played by surface modifiers in the relative weight of both pathways with platinum-modified electrodes, using either a membrane sputtered electrode or with massive ones using flow cell. Valuable properties such as catalyst selectivity and rate constants for the parallel pathways could be evaluated in such experiments.

Acknowledgements

R.N. (# 09/00153-6) and D.A.C. (# 09/11073-3) acknowledge FAPESP for the scholarships. F.H.B.L. (# 08/05156-0 and # 09/07629-6) and H.V. (# 09/07629-6) acknowledge FAPESP for financial support. H.V. acknowledges CNPq for financial support (# 306151/2010-3). R.N. thanks B. C. Batista for fruitful discussions. The authors also acknowledge the referees for helpful comments, and especially Reviewer 2 for the important suggestions concerning the mechanism of methanol electro-oxidation.

References

1 V. S. Bagotzky, Y. B. Vassiliev and O. A. Khazova, *J. Electroanal. Chem.*, 1977, **81**, 229.
2 R. Parsons and T. VanderNoot, *J. Electroanal. Chem.*, 1988, **257**, 9.
3 C. T. Campbell, G. Ertl, H. Kuipers and S. Segner, *J. Chem. Phys.*, 1980, **73**, 5862.
4 H. A. Gasteiger, N. Markovic, P. N. Ross and E. J. Cairns, *J. Phys. Chem.*, 1993, **97**, 12020.
5 S. Sriramulu, T. D. Jarvi and E. M. Stuve, *Electrochim. Acta*, 1998, **44**, 1127.
6 H. Wang, T. Löffler and H. Baltruschat, *J. Appl. Electrochem.*, 2001, **31**, 759.
7 C. Lamy, J.-M. Leger and S. Srinivasan, in *Modern Aspects of Electrochemistry*, ed. J. O. Bockris, B. E. Conway and R. White, Kluwer Academic/Plenum, New York, 2001, vol. 34.
8 N. Markovic and P. N. Ross, *Surf. Sci. Rep.*, 2002, **45**, 117.
9 Y. X. Chen, A. Miki, S. Ye, H. Sakai and M. Osawa, *J. Am. Chem. Soc.*, 2003, **125**, 3680.
10 Z. Jusys, J. Kaiser and R. J. Behm, *Langmuir*, 2003, **19**, 6759.
11 E. A. Batista, G. R. P. Malpass, A. J. Motheo and T. Iwasita, *J. Electroanal. Chem.*, 2004, **571**, 273.
12 D. Cao, G.-Q. Lu, A. Wieckowski, S. A. Wasileski and M. Neurock, *J. Phys. Chem. B*, 2005, **109**, 11622.

13 T. H. M. Housmans, A. H. Wonders and M. T. M. Koper, *J. Phys. Chem. B*, 2006, **110**, 10021.
14 A. Cuesta, *J. Am. Chem. Soc.*, 2006, **128**, 13332.
15 N. A. Anastasijevic, H. Baltruschat and J. Heitbaum, *J. Electroanal. Chem.*, 1989, **272**, 89.
16 Y. E. Seidel, Z. Jusys, R. W. Lindström, M. Stenfeldt, B. Kasemo and K. Krischer, *ChemPhysChem*, 2010, **11**, 1405.
17 O. Wolter and J. Heitbaum, *Ber. Bunsen-Ges. Phys. Chem.*, 1984, **88**, 2.
18 K. Kunimatsu, H. Hanawa, T. Uchida and M. Watanabe, *J. Electroanal. Chem.*, 2009, **632**, 109.
19 M. Osawa, K. Komatsu, G. Samjeske, T. Uchida, T. Ikeshoji, A. Cuesta and C. Gutierrez, *Angew. Chem., Int. Ed.*, 2011, **50**, 1159.
20 A. A. Abd-El-Latif and H. Baltruschat, *J. Electroanal. Chem.*, 2011, **662**, 204.
21 G. Samjeske, A. Miki, S. Ye, A. Yamakata, Y. Mukouyama, H. Okamoto and M. Osawa, *J. Phys. Chem. B*, 2005, **109**, 23509.
22 Y. Mukouyama, M. Kikuchi, G. Samjeske, M. Osawa and H. Okamoto, *J. Phys. Chem. B*, 2006, **110**, 11912.
23 A. Cuesta, G. Cabello, C. Gutierrez and M. Osawa, *Phys. Chem. Chem. Phys.*, 2011, **13**, 20091.
24 S. Sauerbrei, M. A. Nascimento, M. Eiswirth and H. Varela, *J. Chem. Phys.*, 2010, **132**, 154901.
25 D. S. Corrigan and M. J. Weaver, *J. Electroanal. Chem.*, 1988, **241**, 143.
26 J. L. Cohen, D. J. Volpe and H. D. Abruna, *Phys. Chem. Chem. Phys.*, 2007, **9**, 49.
27 K. Krischer and H. Varela, in *Handbook of Fuel Cells–Fundamentals, Technology and Applications*, ed. W. Vielstich, H. A. Gasteiger and A. Lamm, John Wiley & Sons, Chichester, 2003, p. 679.
28 R. P. Buck and L. R. Griffith, *J. Electrochem. Soc.*, 1962, **109**, 1005.
29 M. Hachkar, B. Beden and C. Lamy, *J. Electroanal. Chem.*, 1990, **287**, 81.
30 M. Krausa and W. Vielstich, *J. Electroanal. Chem.*, 1995, **399**, 7.
31 H. Okamoto, N. Tanaka and M. Naito, *J. Phys. Chem. A*, 1997, **101**, 8480.
32 J. Lee, C. Eickes, M. Eiswirth and G. Ertl, *Electrochim. Acta*, 2002, **47**, 2297.
33 W. Vielstich, V. A. Paganin, F. H. B. Lima and E. A. Ticianelli, *J. Electrochem. Soc.*, 2001, **148**, A502.
34 A. L. Martins, B. C. Batista, E. Sitta and H. Varela, *J. Braz. Chem. Soc.*, 2008, **19**, 679.
35 E. A. Carbonio, R. Nagao, E. R. Gonzalez and H. Varela, *Phys. Chem. Chem. Phys.*, 2009, **11**, 665.
36 E. Boscheto, B. C. Batista, R. B. Lima and H. Varela, *J. Electroanal. Chem.*, 2010, **642**, 17.
37 R. Nagao, E. Sitta and H. Varela, *J. Phys. Chem. C*, 2010, **144**, 22262.
38 G. Ertl, *Angew. Chem., Int. Ed.*, 2008, **47**, 3524.

